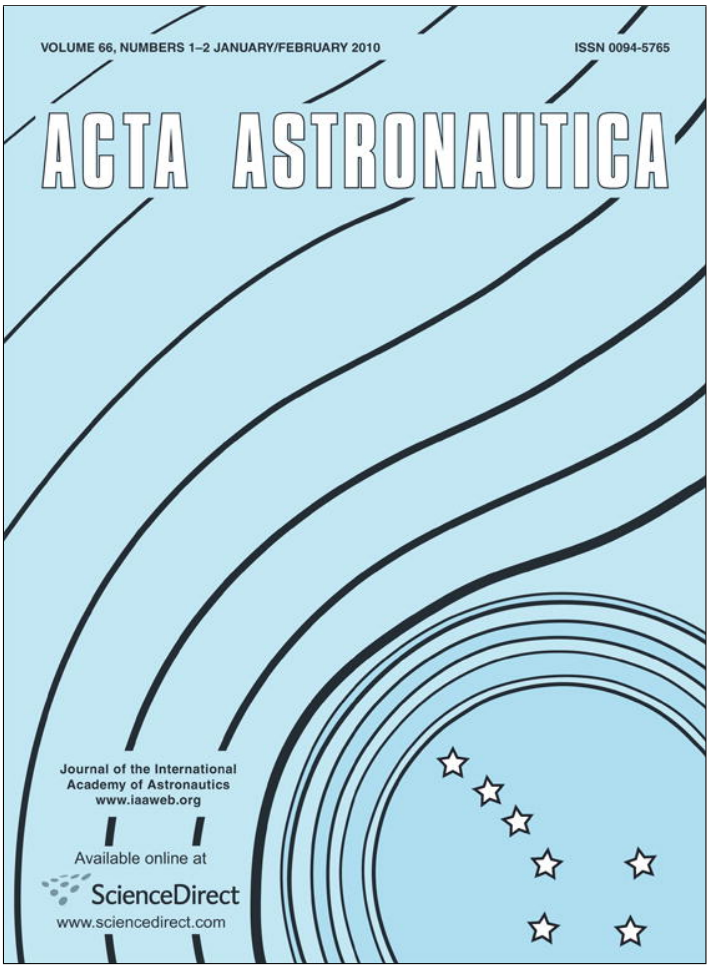

Acta Astronautica 66 (2010) 174 – 182

Contents lists available at ScienceDirect

Acta Astronautica

journal homepage: www.elsevier.com/locate/actaastro

Effects of vibrations on dynamics of miscible liquids

Yu. Gaponenko[a,b], V. Shevtsova[a,*]

[a]Microgravity Research Center, Université Libre de Bruxelles, CP-165/62, Av. F.D. Roosevelt, 50, B-1050 Brussels, Belgium
[b]Institute of Computational Modelling, SB RAS Akademgorodok, 660036 Krasnoyarsk, Russia

ARTICLE INFO

Article history:
Received 19 February 2009
Accepted 23 May 2009
Available online 7 July 2009

Keywords:
Mixing
Vibration
Interface
Miscible fluid

ABSTRACT

We report on a numerical study of the mixing of two miscible fluids in gravitationally stable configuration. In the absence of external forces the diffusion process leads to the mixing of species. The aim of this study is to analyze the physical mechanism by which vibrations affect the mixing characteristic of two stratified miscible fluids. The translational periodic vibrations of a rigid cell filled with different mixtures of water–isopropanol are imposed. The vibrations with a constant frequency and amplitude are directed along the interface. In absence of gravity vibration-induced mass transport is incomparably faster than in diffusion regime. Our results highlight the strong interplay between gravity and vibrational impact, the relative weight of each effect is determined by ratio vibrational and classical Rayleigh numbers.

1. Introduction

Transport phenomena, such as heat and mass transfer, are important in energy production technologies. Here the attention is focused on the mass transfer under vibrations. One of the important industrial applications is mixing in liquids [1]. Two miscible liquids when brought into contact inside a container will mix, i.e. become homogeneous via molecular mass diffusion. Depending on the volume of liquids, spatial homogenization by random molecular motion occurs over a long time scale since the binary diffusion coefficient for liquids is of the order of $10^{-10}\,m^2/s$.

Vibrations, acting on density difference may essentially influence on the fluid dynamics and mass transport. The microgravity environment on-board of ISS is characterized by low mean accelerations, which are 10^{-5}–$10^{-6}g_0$, and fluctuations that are two or three order of magnitude above mean. Interacting with density and concentration gradients, these *g*-jitter may cause convective flows. In weightlessness, it is an additional way of transporting heat and matter similar to thermo- and solutocapillary (Marangoni) convection.

The physical mechanisms by which *g*-jitters affect the mixing characteristics of two miscible fluids initially placed in two vertical regions separated by a thin diffusion layer have been investigated in [2]. Brief study of vibrational impact on behavior of miscible liquids was presented in [3]. They identified four different regimes with increasing of Grashof number: neutral oscillations, successive folds which propagate diffusively; localized shear instability; and both shear and convective instabilities leading to a rapid mixing. The effect of external vibration on the convective flow and heat transfer in a two-layer fluid system of immiscible liquids with density inversion have been investigated in [4]. The effects of external high-frequency vibration on the flow characteristics and interfacial dynamics were examined, and the heat transfer process have been evaluated.

The response of the fluid to external forcing depends on the frequency of vibration. One can speak about low or high frequencies depending on whether the period is

* Corresponding author at: Microgravity Research Center, Université Libre de Bruxelles, CP-165/62, Av. F.D. Roosevelt, 50, B-1050 Brussels, Belgium. Fax: +32 26503126.
E-mail addresses: ygaponen@ulb.ac.be (Yu. Gaponenko), vshev@ulb.ac.be (V. Shevtsova).

0094-5765/$ - see front matter © 2009 Elsevier Ltd. All rights reserved.
doi:10.1016/j.actaastro.2009.05.019

comparable with or much smaller than the reference viscous and heat/mass diffusion times. The high frequency limit is of special interest: here the flow can be represented as a superposition of 'fast' part, which oscillates with the frequency of vibration, and 'slow' time-average part (mean flow), which describes the non-linear response of the fluid to a periodic excitation [5,6].

The choice of the examination of 'mean' flows and application of average approach for this is due to the nature of the considered problem. Because several very different time scales are involved in the process, i.e. viscous time ($\tau_{vis}=L^2/\nu$), diffusion time ($\tau_D=L^2/D$) and period of imposed oscillations, the complexity of simulations can be underestimated. To properly resolve the transport phenomena one should perform calculations with a time step smaller than any of the characteristic physical times, i.e. less than viscous time or period of imposed oscillations. However, mass transport is significantly slower than the viscous process and its characteristic time is determined by diffusion time, $\tau_D \gg \tau_{vis}$. The calculations should cover a long period of physical time, at least by the order of magnitude the final time should be comparable with diffusion time. If someone would like to perform parametric study of physical phenomena in a reasonable CPU time, it might be a problem. Thus instead direct numerical simulations the averaging approach is used, which allow the use of relatively large time steps.

The paper is organized as follows. In Section 2, we explain a model used for numerical simulation. We formulate the problem using non-linear Navier–Stokes and mass transfer equations and describe procedure and validity of the application of the average approach. Results of numerical simulations are given in Section 3.

2. Formulation of the problem

Here the results on numerical modeling of vibrational convection under reduced gravity are presented. The cubic cell of $L=10$ mm length is filled with two miscible liquids: both liquids consist of the same components, water and isopropanol, in different proportions. The layer of heavier/denser liquid (51% of water) is at the bottom and lighter (5% of water) is on the top (gravitationally stable configuration). The system is kept at constant temperature. The direction of vibrations perpendicular to the concentration gradient and coincides with the initial horizontal interface, see Fig 1. Since it is assumed that the two fluids are miscible, there is no discontinuity in the concentration at the interface ($y=\delta L,\ 0<\delta<1$). Because we assumed that interface is sharp, the width of the region over which the initial concentration changes from 1 to 0 is assumed to be 0.03 L.

This system is subjected to periodical oscillations of the cell along the x-axis according to the law $Af(\omega t)$. Here A is vibration amplitude and f is a periodical function:

$$\langle f\rangle = \frac{1}{2\pi}\int_0^{2\pi} f(\tau)\,d\tau = 0.$$

Method utilized herein does not demand specification of the exact type of function f; it can be $\cos(\omega t)$ or $\sin(\omega t)$ or any other periodical function with zero mean value. To simplify notations below let us choose the type of periodicity

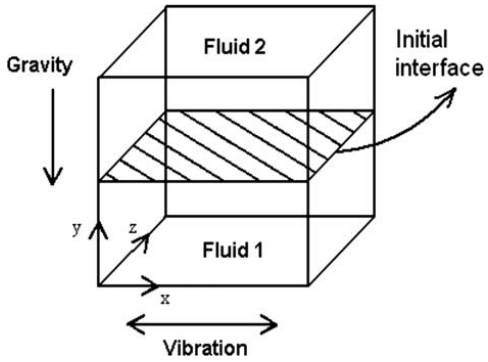

Fig. 1. Geometry of the system.

in such a way, that vibrational velocity and acceleration can be written as

$$v_{os} = A\partial_t f(\omega t) = -A\omega\tilde{f}_1(\omega t),$$

$$a_{os} = -A\omega^2\tilde{f}(\omega t),$$

where $\tilde{f}(\omega t)$ remains a periodical function. In the coordinate system associated with the cell, the acceleration applied to the system is the sum of gravitational and vibrational accelerations:

$$\mathbf{g} + A\omega^2\tilde{f}(\omega t)\mathbf{e},$$

where $\mathbf{g}$ is the constant gravity vector and $\mathbf{e}=(1,0,0)$ is the unit vector along the axis of vibrations.

2.1. Full non-linear equations

The density difference between liquids, i.e. $\Delta\rho$, is assumed to be small, i.e. $\Delta\rho/\rho_0 \ll 1$ and the Boussinesq approximation is valid,

$$\rho = \rho_0(1+\beta_c(C-C_0)).$$

Here $\beta_c=1/\rho_0(\partial\rho/\partial C)$ is the solutal expansion coefficient and C is the concentration of the heavier fluid. It is known that for aqueous solutions of alcohols, the viscosity and the diffusion coefficient are strongly depending on composition. Therefore the viscosity and the diffusion coefficients are considered as function of concentration. Then the equations of motion, mass transport, and continuity can be written as

$$\frac{\partial\mathbf{V}}{\partial t} + (\mathbf{V}\cdot\nabla)\mathbf{V} = -\frac{1}{\rho_0}\nabla P + \nabla(\nu\nabla\mathbf{V}) - \beta_C C[\mathbf{g} + A\omega^2\tilde{f}(\omega t)\mathbf{e}], \quad (1)$$

$$\frac{\partial C}{\partial t} + \mathbf{V}\cdot\nabla C = \nabla(D\nabla C), \quad (2)$$

$$\operatorname{div}\mathbf{V} = 0. \quad (3)$$

Here $\mathbf{V}$ is the vector of velocity, P is the pressure, D is the molecular diffusion, ν is the kinematic viscosity, and $P=P'-g_0\rho_0 y$ is the pressure. All reference values, noted by subscript '0' are taken at the equilibrium conditions, i.e. the mean values for two mixtures at the initial state.

Let us introduce dimensionless variables by taking the scales of length L, time L^2/ν, velocity ν/L, pressure $\rho_o \nu^2/L^2$, and initial concentration difference Δc. The dimensionless equations are written in the form

$$\partial_t \mathbf{v} + (\mathbf{v}\cdot\nabla)\mathbf{v} = -\nabla P + \nabla\left(\frac{\nu}{\nu_0}\nabla\mathbf{v}\right) - Sc^{-1}[Ra + Ra_{os}\tilde{f}(\omega t)\mathbf{e}]c, \quad (4)$$

$$\partial_t c + \mathbf{v}\cdot\nabla c = Sc^{-1}\nabla\left(\frac{D}{D_0}\nabla c\right), \quad (5)$$

$$\operatorname{div}\mathbf{v} = 0, \quad (6)$$

where $c = (C - C_0)/\Delta c$ and C_0 is the initial concentration of heavier liquid. The system includes the Rayleigh number Ra, the oscillatory Rayleigh number Ra_{os}, the Schmidt number Sc, the dimensionless angular frequency Ω:

$$Ra = \frac{g\beta_c \Delta c L^3}{\nu_0 D_0}, \quad Ra_{os} = \frac{A\omega^2\beta_c \Delta c L^3}{\nu_0 D_0},$$

$$Sc = \nu_0/D_0, \quad \Omega = \omega L^2/\nu_0. \quad (7)$$

The cell boundaries are rigid with no-slip condition for the velocity and no-penetration for concentration

$$\mathbf{v} = 0, \quad \partial_{\mathbf{n}} c = 0, \quad (8)$$

where $\mathbf{n}$ is the normal vector to the rigid walls. An additional parameter of the problem, the initial position of the interface, δ, enters to the initial conditions. The initial conditions correspond to zero velocity and constant concentration in each layer of fluid: $\mathbf{V} = 0$; $C = 1$, for $0 \le y < \delta$ and $C = 0$ for $\delta \le y < 1$.

2.2. Averaging approach

In the limit of high frequency and small amplitude of periodical vibration the averaging method can be applied effectively to study the property of vibrational convection, see, e.g. [5,6]. The averaging procedure is rather confusing and for better understanding we will give some details. According to this method each field is subdivided into two parts: slow (the characteristic time is large with respect to the vibration period) and fast(the characteristic time is of the order of the vibration period) parts

$$\mathbf{V} = \overline{\mathbf{V}} + \mathbf{V}', \quad P = \overline{P} + P', \quad C = \overline{C} + C', \quad (9)$$

here $(\overline{\mathbf{V}}, \overline{P}, \overline{C})$ are the slow (averaged) components and $(\mathbf{V}', P', C')$ are the fast (oscillating) components. Let us substitute relations (9) into Eqs. (1)–(3) and consider the fast fields:

$$\partial_t \mathbf{V}' + (\overline{\mathbf{V}}\cdot\nabla)\mathbf{V}' + (\mathbf{V}'\cdot\nabla)\overline{\mathbf{V}} + (\mathbf{V}'\cdot\nabla)\mathbf{V}' = -\rho_0^{-1}\nabla P' + \nabla(\nu\nabla\mathbf{V}') - \mathbf{g}\beta_C C' + \beta_C(\overline{C} + C')A\omega^2\tilde{f}(\omega t)\mathbf{e}, \quad (10)$$

$$\partial_t C' + (\overline{\mathbf{V}}\cdot\nabla)C' + (\mathbf{V}'\cdot\nabla)\overline{C} + (\mathbf{V}'\cdot\nabla)C' = \nabla(D\nabla C'), \quad (11)$$

$$\nabla\cdot\mathbf{V}' = 0. \quad (12)$$

The mean (slow) fields in this formulation have the same scaling, as the corresponding quantities in Eqs. (4)–(6). The length scale L remains the same. The fast time is scaled with the period of oscillations $\tau_{os} = 2\pi/\omega$. For the fast fields, defined on 'quick' time, a new scaling is introduced with subscript 's'

$$\tilde{t} = \frac{t}{\tau_{os}}, \quad \tilde{\mathbf{V}} = \frac{\mathbf{V}'}{\nu_s}, \quad \tilde{C} = \frac{C'}{C_s}, \quad \tilde{P} = \frac{P'}{P_s}. \quad (13)$$

Using these scales Eqs. (10)–(12) will be written as (for mean values the same notations are used to avoid multiplying of notations)

$$\frac{V_s}{\tau_{os}}\frac{\partial\tilde{\mathbf{V}}}{\partial\tilde{t}} + \frac{\nu_0 V_s}{L^2}[(\overline{\mathbf{V}}\cdot\nabla)\tilde{\mathbf{V}} + (\tilde{\mathbf{V}}\cdot\nabla)\overline{\mathbf{V}}] + \frac{V_s^2}{L}(\tilde{\mathbf{V}}\cdot\nabla)\tilde{\mathbf{V}} = -\frac{P_s}{\rho_0}\nabla\tilde{P} + \frac{\nu_0 V_s}{L^2}\nabla\left(\frac{\nu}{\nu_0}\nabla\tilde{\mathbf{V}}\right) - \mathbf{g}\beta_C C_s\tilde{C} + \beta_C(\overline{C}\,\Delta C + \tilde{C}C_s)A\omega^2\tilde{f}(\omega t)\mathbf{e}, \quad (14)$$

$$\frac{V_s}{\tau_{os}}\frac{\partial\tilde{C}}{\partial\tilde{t}} + \frac{\nu_0 C_s}{L^2}(\overline{\mathbf{V}}\cdot\nabla)\tilde{C} + \frac{V_s\Delta C}{L}(\tilde{\mathbf{V}}\cdot\nabla)\overline{C} + \frac{V_s C_s}{L}(\tilde{\mathbf{V}}\cdot\nabla)\tilde{C} = \frac{D_0 C_s}{L^2}\nabla\left(\frac{D}{D_0}\nabla\tilde{C}\right). \quad (15)$$

The fast scales will be chosen later in such a way that only the main terms will be kept in the equations for the fast fields:

$$\partial_t\mathbf{V}' = -\rho_0^{-1}\nabla P' - \beta_C\overline{C}A\omega^2\tilde{f}(\omega t)\mathbf{e}, \quad (16)$$

$$\partial_t\mathbf{C}' = -(V'\cdot\nabla)\overline{C}, \quad (17)$$

$$\nabla\cdot V' = 0. \quad (18)$$

2.2.1. Choice of characteristic scales for the fast fields

By choosing new temporal scales we will introduce limitations, at which the averaging approach correctly describes the phenomenon of thermo-vibrational convection.

(a) In the left-hand side of Eq. (16) only the derivative with respect to 'quick' time is kept, so the following conditions are imposed

$$\frac{V_s}{\tau_{os}} \gg \frac{\nu_0 V_s}{L^2} \quad \text{and} \quad \frac{V_s}{\tau_{os}} \gg \frac{V_s^2}{L}$$

$$\rightarrow \tau_{os} \ll \frac{L^2}{\nu_0}, \quad V_s \ll \frac{L}{\tau_{os}}.$$

(b) In the right-hand side we neglect by the viscous term

$$\frac{V_s}{\tau_{os}} \gg \frac{\nu_0 V_s}{L^2} \rightarrow \tau_{os} \ll \frac{L^2}{\nu_0}.$$

(c) In addition in the right-hand side we neglect by the buoyancy force $\beta_C C'\mathbf{g}$. First, we demand that amplitude of concentration oscillations is small, i.e. $C_s \ll \Delta C$ and then that buoyancy force is smaller than vibrational force

$$g\beta_C C_s \ll \beta_C \Delta C A\omega^2 \rightarrow C_s \ll A\omega^2\,\Delta C/g.$$

(d) Applying the similar procedure for the mass transport equation an additional assumptions are introduced. For illumination of convective terms

$$\frac{C_s}{\tau_{os}} \gg \frac{v_0 C_s}{L^2} \quad \text{and} \quad \frac{C_s}{\tau_{os}} \gg \frac{V_s C_s}{L} \rightarrow \tau_{os} \ll \frac{L}{V_s}.$$

(e) For neglecting by mass diffusion

$$\frac{C_s}{\tau_{os}} \gg \frac{D_0 C_s}{L^2} \rightarrow \tau_{os} \ll \frac{L^2}{D_0}.$$

Taking into account *a*, *b*, *c*, *d*, *e* the assumptions of averaging approach can be formulated:

1. The limitation for high frequency vibrations follow from points *a*, *b*, *e*, written above, i.e. the period of external vibrations (τ_{os}) must be small with respect to all characteristic times. Simultaneously, the Boussinesq model of an incompressible fluid requires that the acoustic wavelength must be larger than the characteristic length scale. Then the vibration period is to satisfy

$$\frac{L}{c} = \tau_{sound} \ll \tau_{os} \ll \min\left[\tau_{vis} = \frac{L^2}{\nu}, \tau_D = \frac{L^2}{D}\right].$$

The viscous time is smaller than the diffusion time, $\tau_{vis}/\tau_{th} = 1/Pr$. Thus, the limitations for the frequency is based on the viscous time, i.e. the dimensionless frequency Ω is

$$\Omega = \frac{\omega L^2}{\nu} \gg 1. \tag{19}$$

2. In the left-hand side of Eq. (16) we also neglected by the non-linear terms $(\mathbf{V}'\cdot\nabla)\mathbf{V}'$ and $(\overline{\mathbf{V}}\cdot\nabla)\mathbf{V}'$, $(\mathbf{V}'\cdot\nabla)\overline{\mathbf{V}}$. It means, that displacement amplitude is sufficiently small

$$A \ll \frac{L}{\beta_C \Delta C} \quad \text{or} \quad \frac{A}{L} \ll \frac{1}{\beta_C \Delta C},$$

but may be larger than cell size; usually $\beta_C \Delta C < 1$. Besides, we neglected in equation for the 'quick' component of the flow by the gravitational buoyancy force $\beta_C C'\mathbf{g}$. It is justified under the following relationship between the gravity and the vibrational accelerations

$$\frac{g}{A\omega^2}\frac{A}{L}\beta_C \Delta C \ll 1 \quad \text{or} \quad \frac{g}{L\omega^2}\beta_C \Delta C \ll 1.$$

2.2.2. Solving equations for the fast fields

To solve Eq. (16) the vector $\overline{C}\,\mathbf{e}$ is decomposed as

$$\overline{C}\mathbf{e} = \mathbf{W} + \nabla\Phi, \quad \nabla\cdot\mathbf{W} = 0, \tag{20}$$

where $\mathbf{W}$ is its solenoidal part and $\nabla\Phi$ is its potential part. Substituting (20) into Eq. (16) one will get

$$\partial_t \mathbf{V}' = -\beta_C A\omega^2 \tilde{f}(\omega t)\mathbf{W}, \tag{21}$$

$$\rho_0^{-1}\nabla P' = -\beta_C A\omega^2 \tilde{f}(\omega t)\nabla\phi. \tag{22}$$

Integrating these equations over the 'quick' time, then substituting solution to Eq. (17), one may write the resulting relations for the fast components

$$\mathbf{V}' = -\beta_C A\omega \mathbf{W}\tilde{f}_1(\omega t), \tag{23}$$

$$C' = -\beta_C A(\mathbf{W}\cdot\nabla\overline{C})f(\omega t), \tag{24}$$

$$P' = -\beta_C \rho_0 A\omega^2 \Phi\tilde{f}(\omega t). \tag{25}$$

These equations define the characteristic scales of oscillatory fields

$$V' \sim \beta_C \Delta C A\omega,$$

$$C' \sim \beta_C \Delta C^2 A/L,$$

$$P' \sim \beta_C \rho_0 A\omega^2 \Delta C. \tag{26}$$

Note, that if $f=\cos(\omega t)$ in Eqs. (23)–(25), then $\tilde{f}_1(\omega t)=\sin(\omega t)$ and $\tilde{f}(\omega t) = \cos(\omega t)$.

2.2.3. Equation for mean fields

On the next step we will write equation for the averaged quantities. Substituting (23)–(25) into the complete set of equations and integrating (averaging) over the fast time, we will obtain the governing equation for the mean fields

$$\frac{\partial\overline{\mathbf{V}}}{\partial t} + (\overline{\mathbf{V}}\cdot\nabla)\overline{\mathbf{V}} = -\frac{1}{\rho_0}\nabla\overline{P} + \nabla\left(\frac{\nu}{\nu_0}\nabla\overline{\mathbf{V}}\right) - \beta_C\overline{C}\mathbf{g} + \frac{(\beta_C A\omega)^2}{2}[(\mathbf{W}\cdot\nabla)(\overline{C}\mathbf{e} - \mathbf{W})], \tag{27}$$

$$\frac{\partial\overline{C}}{\partial t} + (\overline{\mathbf{V}}\cdot\nabla)\overline{C} = D_0\nabla\left(\frac{D}{D_0}\nabla\overline{C}\right), \tag{28}$$

$$\nabla\cdot\mathbf{V} = 0, \quad \mathbf{W} = \overline{C}\mathbf{e} - \nabla\Phi, \quad \operatorname{div}\mathbf{W} = 0. \tag{29}$$

The characteristic scale for $\mathbf{W}$, Φ are ΔC and $\Delta C/L$, ($\varphi = \Phi\,\Delta C\,L$). Using for other slow and fast quantities the characteristic scales, introduced above, the non-dimensionless form of the governing equations can be written as (we omit here overline for *mean*)

$$\frac{\partial\mathbf{v}}{\partial t} + \mathbf{v}\cdot\nabla\mathbf{v} = -\nabla p + \nabla\left(\frac{\nu(c)}{\nu_0}\nabla\mathbf{v}\right) + Sc^{-1}[-Ra\,c + Gs((c\mathbf{e} - \nabla\varphi)\nabla)\nabla\varphi],$$

$$\frac{\partial c}{\partial t} + \mathbf{v}\cdot\nabla c = Sc^{-1}\nabla\left(\frac{D(c)}{D_0}\nabla c\right),$$

$$\operatorname{div}\mathbf{v} = 0, \quad \mathbf{w} = c\mathbf{e} - \nabla\varphi, \quad \operatorname{div}\mathbf{w} = 0. \tag{30}$$

Here Rayleigh number, *Ra*, characterizes gravitational mechanism of convection and *Gs* is its vibrational analogue:

$$Gs = Ra_{vib} = \frac{(A\omega\beta_C \Delta C L)^2}{2\nu D_0} \tag{31}$$

and describes the vibrational mechanism of convection represented by the mean flow. We suggest to call it Gershuni number (instead of vibrational Rayleigh number Ra_{vib}) to mark a significant contribution of Gershuni to the theory of thermovibrational convection [6]. Note, that Ra_{os}, introduced

Table 1
Physical properties of the initial water/isopropanol mixtures.

c	$\nu_0 \times 10^6$ (m^2/s)	β_c	$D_0 \times 10^{10}$ (m^2/s)	$\rho_0 \times 10^{-3}$ (kg/m^3)	Sc
0.05	3.08	0.213	7.778	0.795	3957
0.51	4.17	0.187	1.86	0.902	23 167
0.28	3.99	0.203	2.70	0.853	14 778

Last raw corresponds to the 'mean' values of top and bottom mixtures.

earlier in Eq. (7) characterizes the physics of full flow, but *does not* describes properly the 'mean' fields.

2.3. Governing equations

The target of this study is to examine the mixing of realistic fluid, when the Schmidt number is very large, $Sc = 14\,778$ (see Table 1). For this purpose, we will restrict our study by 2D calculations and converse the problem into stream-function vorticity formulation. For the mean fields a stream function, ψ, such that $v_x = \partial\psi/\partial y, v_y = -\partial\psi/\partial x$ and a vorticity, $\zeta = \partial v_y/\partial x - \partial v_x/\partial y$ are introduced. Eqs. (30) for mean fields are rewritten in the form

$$\frac{\partial\zeta}{\partial t} + \frac{\partial\psi}{\partial y}\frac{\partial\zeta}{\partial x} - \frac{\partial\psi}{\partial x}\frac{\partial\zeta}{\partial y} = \nabla\left(\frac{\nu(c)}{\nu_0}\nabla\zeta\right) - \frac{Ra}{Sc}\frac{\partial c}{\partial x} + \frac{Gs}{Sc} \times \left(\frac{\partial c}{\partial y}\frac{\partial^2\varphi}{\partial x^2} - \frac{\partial c}{\partial x}\frac{\partial^2\varphi}{\partial x\partial y}\right), \quad (32)$$

$$\frac{\partial c}{\partial t} + \frac{\partial\psi}{\partial y}\frac{\partial c}{\partial x} - \frac{\partial\psi}{\partial x}\frac{\partial c}{\partial y} = Sc^{-1}\nabla\left(\frac{D(c)}{D_0}\nabla c\right), \quad (33)$$

$$\nabla^2\psi = -\zeta, \quad \nabla^2\varphi = -\frac{\partial c}{\partial x}. \quad (34)$$

The boundary conditions could be written in the form

$$x = 0, 1 : \psi = \partial_x\psi = 0, \quad \partial_x c = 0, \quad \partial_x\varphi = c,$$

$$y = 0, 1 : \psi = \partial_y\psi = 0, \quad \partial_y c = 0, \quad \partial_y\varphi = 0.$$

The conditions for φ follows from non-permeability conditions for the vector field $\mathbf{W}\cdot\mathbf{n}|_\Gamma = 0$ on the rigid boundary Γ. Note that the viscous force driving the oscillatory flow has been neglected when deriving Eq. (16). The initial conditions are

$$t = 0 : \psi = \zeta = 0, \quad \partial_x c = 0,$$

$$c = 1 \quad \text{when } 0 \le y < \delta,$$

$$c = 0 \quad \text{when } \delta < y \le 1,$$

$$\partial_x\varphi = c; \quad \partial_y\varphi = 0.$$

The physical properties, used in calculations, are listed in Table 1. Last line corresponds to the mixture when the initial interface is at mid-height.

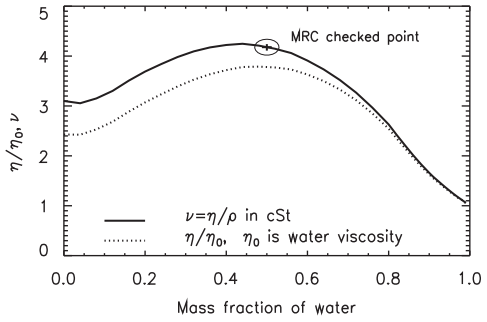

Fig. 2. Viscosity, $\nu = \nu(C)$, of water/isopropanol mixture.

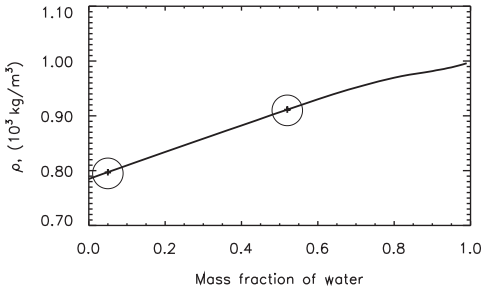

Fig. 3. Density, $\rho = \rho(C)$, of water/isopropanol mixture.

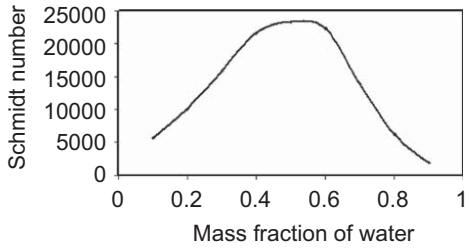

Fig. 4. Dependence of Schmidt number, $Sc = \nu/D$, on concentration of water/isopropanol mixture.

A finite-difference method in both directions is utilized. The time derivatives are forward differenced and for the convective and diffusive terms are central approximated. The Poisson equation for the stream function ψ and for the amplitude φ of fast pressure were solved by introducing an artificial iterative term, analogous to the time-derivative one. ADI method is used to solve the time-dependent problem for vorticity, the concentration, the pulsatory pressure amplitude, and the stream function. More detail about numerical procedure one may find in [7].

The dependence of density, $\rho(C)$, and viscosity, $\nu(C)$, for water–isopropanol mixture was found in handbooks [8]. One of the points on the viscosity curve was verified experimentally, see Fig. 2. The value of β_C in Table 1 was estimated according to Fig. 3. Data for diffusion, $D(c)$, are somewhat scattered and they were taken from different sources [9,10]. They were used for estimation of the Schmidt number shown in Fig. 4.

The explicit form of the dependences $v(C)$ and $D(C)$ used in calculations was obtained on the basis of mentioned above dependencies:

$$v(C) = (90.092C^6 - 264.46C^5 + 312.43C^4 - 192.57C^3 + 54.93C^2 - 2.486C + 3.0901) \times 10^{-6}\ \mathrm{m^2/s},$$

$$D(C) = (18.189 * C^4 - 33.6193 * C^3 + 23.672 * C^2 - 7.694 * C + 1.180) \times 10^{-10}\ \mathrm{m^2/s}.$$

3. Results

Translational vibrations act on the non-uniformity of density and generate the oscillatory convection. In the considered geometry, the problem is governed by four parameters: the Schmidt number, Sc, the Rayleigh number, Ra, the Gershuni number, Gs (or its analog vibrational Rayleigh number Ra_{vib}) and the initial interface location δ. Different flow regimes were observed depending on the ratio of these parameters. The general trend of the flow development is the following: convection starts at the cross-section of the interface with solid walls. To present results of this multiparametric problem some of the parameters will be frozen, e.g. thickness of both liquids is taken equal. We will consider initially gravitationally stable system composed of two miscible mixtures. Initial compositions are: 5% water–95% isopropanol at the top and 51% water–49% isopropanol at the bottom. These mixtures are encircled on density curve in Fig. 3.

3.1. Net and mean flow

First, we would like to draw your attention to the difference between net fields described by Eqs. (1)–(3) and mean fields described by Eq. (32)–(34). The net flow consists of one vortex, which occupies the whole system and rotates to one side for a half of the period and to the opposite side for another half of the period, see Fig. 5a. For relatively strong external excitations (see Eq. (19)) the fluid cannot immediately return to its initial position due to inertia and convective mean flow is created. The vibrations organize mean flow in such a way that heavy/denser liquid moves up along the both solid walls, x=0 and 1 and less dense moves down. Two weak vortexes with the opposite direction of the circulation are formed in each fluid, see Fig. 5b. Hereafter we consider only the cases, for which all theoretical requirements for existence of this mean flow are fulfilled. Further presentation will be given for dimensionless concentration: at the beginning concentration of heavier/denser liquid at the bottom is $c_0 = 1$ and the concentration of top liquid is $c_0 = 0$.

The temporal behavior of the interface is shown in Fig. 6 shortly after beginning of flow development. The position of interface is defined as a collection of concentration isolines, where the levels change from $c = 0.9$ to 0.1. The interface is swinging around some mean position with the frequency of imposed oscillations. Hereafter we will show only 'mean' position, i.e. 'mean' field defined by Eq. (9). The evolution of the mass transfer with time strongly depends on the ratio of parameters.

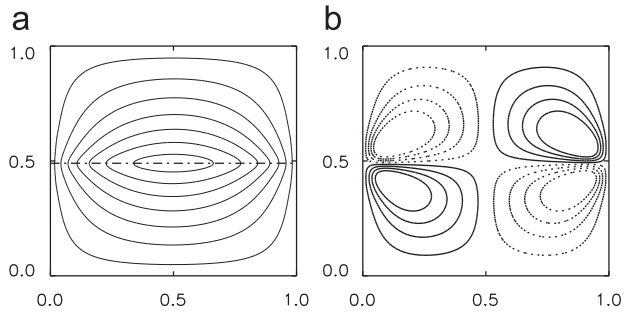

Fig. 5. The flow structure (isolines of ψ) at the very beginning ($t = 1$) for $Sc_0 = 14\,778$, $Ra = 0$ ($g = 0$), $Gs = 7.86 \times 10^7$. (a) Snapshot of the full flow and (b) mean flow.

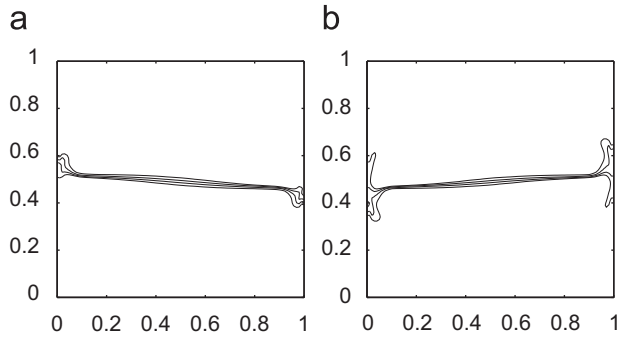

Fig. 6. The interface location (isolines of full c) at the very beginning for $Sc_0 = 14\,778$, $Ra = 0$ ($g = 0$), $Gs = 7.86 \times 10^7$ at two different time moment.

3.2. Absence of gravity, $Ra = 0$

The 'effective' Schmidt number (mean value for both liquids) is $Sc_0 = 14\,778$, see Table 1. The vibrational effect is fixed: $Gs = 7.86 \times 10^7$, which corresponds to the following parameters of the experiment: $f = 8$ Hz, $A = 1$ cm, $\Delta c = 0.46$. Here we will discuss the fluid behavior in the upper liquid until it is not stated otherwise. From the very beginning, the concentration front moves along the solid walls, creating a head, see Fig. 7 ($t = 0.1$–5). The leading part of the front (this notation is used for isolines $c = 0.7$) expands and rolls up, and a denser liquid intrudes into the less dense region, see Fig. 7 ($t = 5$). The flow resembles a Kelvin–Helmholtz instability which is observed in free shear layers and gravity currents. The instability appears almost immediately after imposing vibrations and persists during certain interval of time. For example, for $Ra = 0$ it exists up to 10 viscous times. The horizontal solid walls impose constrains on the approaching concentration front and it turns inside the cell creating another flow organization, when the denser liquid is on top of the less dense.

This scenario is a kind of Rayleigh–Taylor instability, which is observed in ground conditions (when heavy liquid is on the top). Further the denser liquid starts to descend, and it splits the region of low concentration in a few zones, see Fig. 7 ($t = 20$).

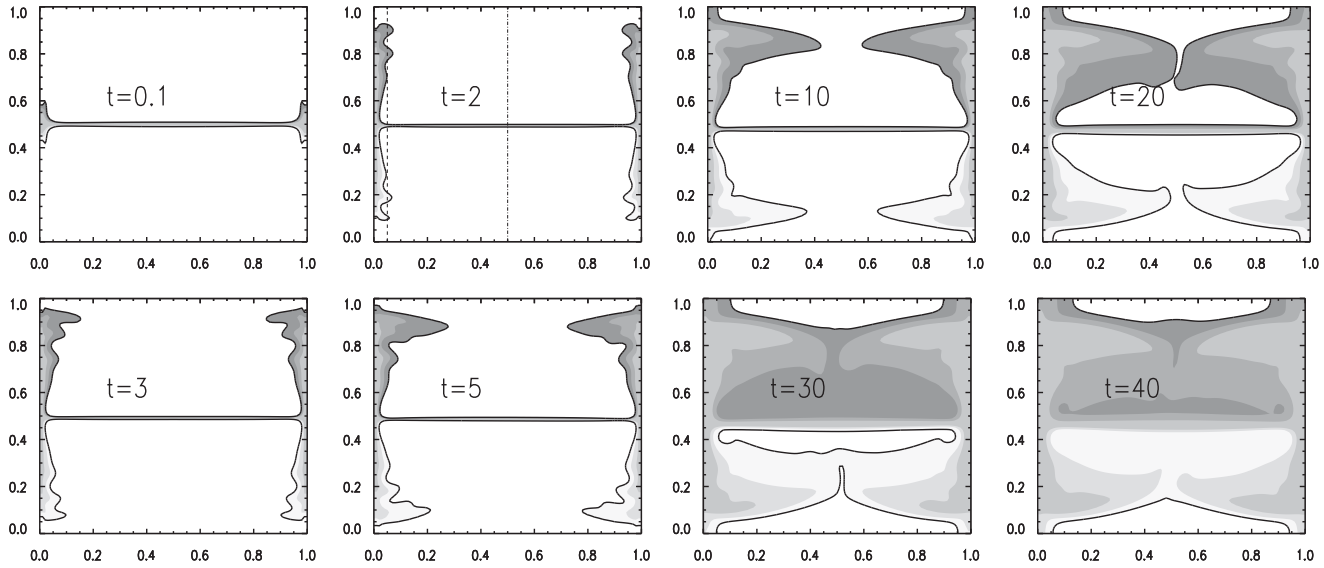

Fig. 7. Evolution of the concentration front; The leading profiles are $c=0.3$ and 0.7 at lower and upper liquid, correspondingly. Shadowed space corresponds to the intermediate concentration region $0.29 < c < 0.71$. Dimensionless time inside the graphs is given in viscous times, $\tau_{vis} = L^2/\nu$, $Ra = 0$.

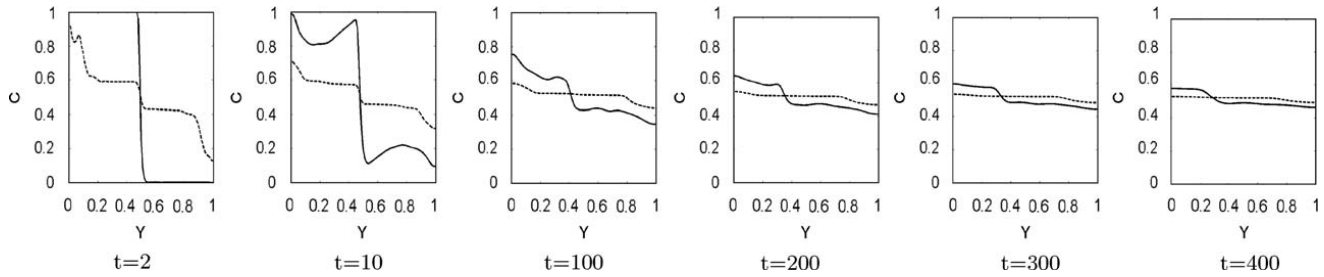

Fig. 8. Evolution of the vertical concentration profile with time; solid and dashed lines show concentration $c(y)$ in the middle ($x = 0.5$) and near the wall ($x = 0.05$), respectively.

The flow is not exactly similar in the upper and lower fluids. The break of symmetry is related to the non-linear dependence of the viscosity and the diffusion coefficients on concentration. Note, that during relatively long time over which Kelvin–Helmholtz and Rayleigh–Taylor instabilities develop, the role of diffusion is undetectable. The major part of the interface remains almost as sharp as in the initial stage.

One may follow the development of mixing process on long time scale analyzing the behavior of curves in Fig. 8. The solid and dashed lines show vertical concentration profiles $c(y)$ in the middle ($x = 0.5$) and near the wall ($x = 0.05$). For better understanding, the lines, along which the concentration profiles are shown, are displayed in Fig. 7 ($t = 2$) by vertical lines. For the first 10 viscous times, the initial concentration distribution in the middle (solid line) is not affected by vibrations while near-wall regions the liquid is almost homogeneous. It is worth to emphasize, that the fast mixing process essentially homogenizes mixture at about 100 viscous times. Later in time, the mixing is much slower and at $t = 400$ almost complete mixing is achieved. The smaller is the concentration non-uniformity, the weaker is convection produced by vibrations.

It is interesting to compare diffusive and vibration-induced mixing times scales. The diffusion time, $\tau_D = L^2/D$ is shown in Fig. 9 by curve with rhombus. The curve with triangles displays dependence of mixing time on concentration multiplied by factor 400(!), i.e. the time when mixing by vibrations is completed according to Fig. 8. In both curves the time is measured in viscous times $t = L^2/\nu$. Assuming that mixing by diffusion can be achieved during one diffusion time, we conclude that the vibrational mechanism is significantly faster.

Let us look at the dynamics of the flow which provides mass transport of the liquids. When heavy liquid climbing along the wall achieves the upper horizontal wall, the mean flow (streaming) becomes oscillatory. It starts at $t \approx 7$–10 viscous times. The flow pattern in two different time moments ($t = 27$ and 30, respectively) are shown in Fig. 10. It clearly shows change in flow direction with time. For the examined set of parameters, the amplitudes of velocity and of concentration oscillations decay extremely slowly with time. Time history of stream function at two points, being located at two different vortexes in Fig. 10, are shown in Fig. 11. Stream function oscillates with period about six viscous times and its amplitude slowly decreases.

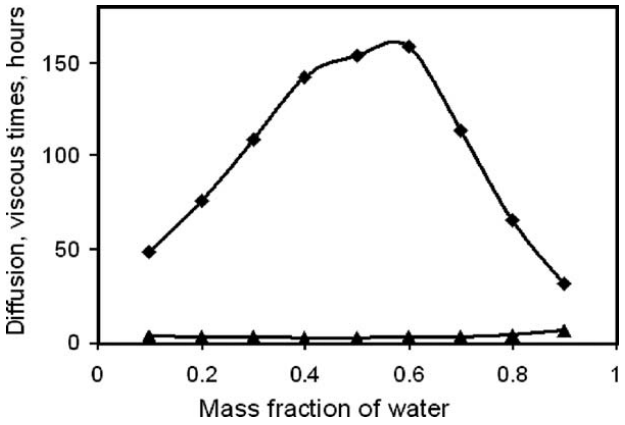

Fig. 9. Curve with rhombus shows diffusion time, $t = \tau_D = L^2/D$ for water/isopropanol mixture; Curve with triangles outlines mixing time (magnified by 400) in presence of vibration. In both curves the time is measured in viscous times $t = L^2/\nu$.

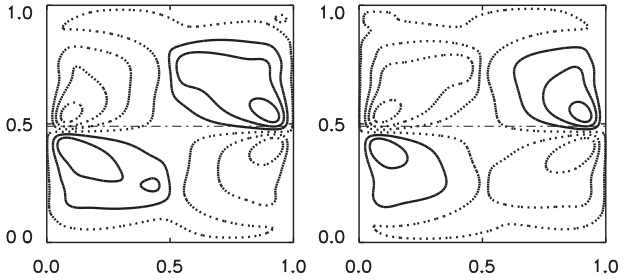

Fig. 10. Oscillations of mean flow; Isolines of ψ at $t = 27$ and 30.

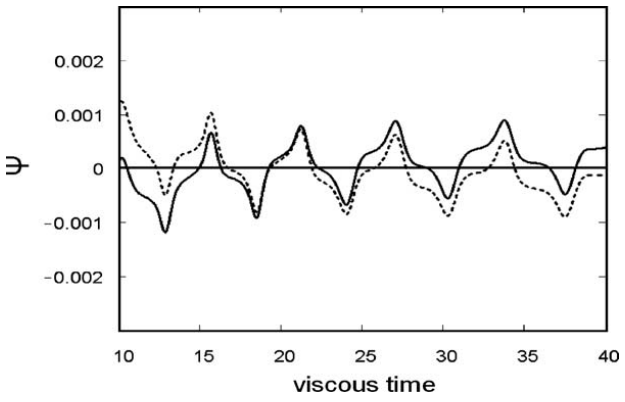

Fig. 11. Time history of stream function in two fixed points in the bulk: $(x,y) = (0.37, 0.9)$ is shown by solid line and $(x,y) = (0.65, 0.9)$ is shown by dotted line.

3.3. *Effect of gravity, $Ra \neq 0$*

With appearing of gravity field the flow dynamic, described above, is changing. The concentration front rolls up with a decreasing velocity: the larger the gravity, the smaller the velocity. One may compare the propagation of mixing front in Figs. 7 and 12 at the same time instant. As all parameters of system were fixed we may say by other words that

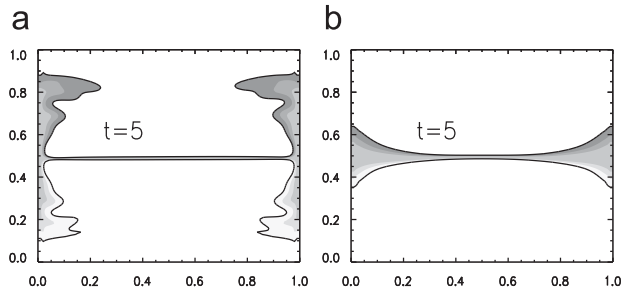

Fig. 12. Evolution of the concentration front in the same time moment for different gravity levels when $Sc = 14\,778$, $Gs = 7.86 \times 10^7$. (a) $Ra = 1.69 \times 10^7$, $g/g_0 = 0.026$ and (b) $Ra = 1.13 \times 10^8$, $g/g_0 = 0.173$.

graphs in Fig. 12 correspond to the gravity level $g/g_0 = 0.026$ and 0.1737. Here g_0 is the Earth gravity.

With increasing gravity the intrusion of denser liquid along the wall slows down. In the latter case, $Ra = 1.13 \times 10^8$, (see Fig. 12b) the upward motion of denser liquid is stopped by the gravity and Kelvin–Helmholtz instability does not set-in. Here the ratio of Rayleigh numbers is about $Ra/Gs = 1.44$. Thus, when the classical Rayleigh number becomes comparable or larger with the vibrational one, the Kelvin–Helmholtz instability is not observed. For the picture in Fig. 12a the ratio is $Ra/Gs = 0.215$.

We may draw a conclusion that the vibrations are the driving mechanism for this instability and the local mixing along the solid walls.

4. Conclusions

We have investigated the physical mechanism by which external vibrations affect the mass transfer between two miscible fluids which were initially separated by a thin (vertically) diffusion layer. The translational periodic vibrations of a rigid cell filled with different mixtures of water–isopropanol are imposed. The vibrations with a constant frequency and amplitude are directed along the interface. The mean fields of flow and concentration, caused by vibrations and buoyancy, were examined. Our results highlight the strong interplay between gravity and vibrational impact. For the parameter set, where vibrational mechanism dominates, the Kelvin–Helmholtz instability produces vortices near solid walls which can serve as a stirring mechanism to promote local mixing. The Rayleigh–Taylor instability strongly affects on large scale mixing. If the gravity forcing is dominant the mixing occurs much more slowly, on the diffusion time scale.

For high frequency oscillations the averaged approach, adopted in this study, is beneficial. The larger time step can be employed and the observation can be easily done on the long time scale, i.e. up to 400 viscous times.

Acknowledgments

This work is supported by the PRODEX programme of the Belgian Federal Science Policy Office. The authors thank Prof. J.C. Legros, whose comments substantially improved the presentation of the results.

References

[1] T. Nishimura, Y.N. Bian, K. Kunitsugu, Mass-transfer enhancement in a wavy-walled tube by imposed fluid oscillation, AIChE J. 50 (2004) 762–770.
[2] V.K. Siddavaram, G.M. Homsy, Effects of gravity modulation on fluid mixing. Part 1. Harmonic modulation, J. Fluid Mech. 562 (2006) 445–475.
[3] Yu. Gaponenko, V. Shevtsova, Mixing under vibrations in reduced gravity, Microgravity Sci. Technol. 20 (2008) 307–311.
[4] Q. Chang, J.I. Alexander, Thermal vibrational convection in a two-phase stratified liquid, C. R. Mec. 335 (2007) 304–314.
[5] S.M. Zenkovskaya, I.B. Simonenko, On the effect of high-frequency vibrations on the origin of convection, Izv. AN SSSR Ser. Mekh. Zhidk. i Gaza. (5) (1965) 51–55.
[6] G.Z. Gershuni, D.V. Lyubimov, Thermal Vibrational Convection, Wiley, England, 1998.
[7] Yu.A. Gaponenko, J.A. Pojman, V.A. Volpert, S.M. Zenkovskaja, Effect of high-frequency vibration on convection in miscible liquids, J. Appl. Mech. Tech. Phys. 47 (2006) 49–59.
[8] D.R. Lide, CRC Handbook of Chemistry and Physics, 74th ed., CRC, London, 1993.
[9] K.C. Pratt, W.A. Wakeham, Proc. R. Soc. London Ser. A Math. Phys. Sci. 336 (1974) 393–406.
[10] A. Mialdun, V. Shevtsova, Development of optical digital interferometry technique for measurement of thermodiffusion coefficients, Int. J. Heat Mass Transfer 51 (2008) 3164.